

Photophysics of Aminoxanthone Derivatives and Their Application as Binding Probes for DNA[†]

Tamara C. S. Pace, Sarah L. Monahan, Andrew I. MacRae, Monica Kaila and Cornelia Bohne*

Department of Chemistry, University of Victoria, Victoria, BC, Canada

Received 16 May 2005; accepted 08 August 2005; published online 12 August 2005 DOI: 10.1562/2005-05-16-RA-529

ABSTRACT

Xanthenes with amino substituents were synthesized to diminish the photoreactivity of the xanthone chromophore with DNA, with the objective of using these molecules to study their binding dynamics with DNA. The aminoxanthenes showed a strong solvatochromic effect on their singlet and triplet excited-state photophysics, where polar solvents led to a decrease of the energies for the excited states. Quenching of the triplet excited states by nitrite anions was used to determine the binding dynamics, and a residence time in the microsecond time domain was estimated for the bound 2-aminoxanthone with DNA. The quenching experiments performed showed that this methodology will not be applicable to study the binding dynamics of a wide variety of guests with DNA.

INTRODUCTION

Dynamics play a key role in the function of complex systems in chemistry and biology, such as ion transport and catalysis. The biological activity of antitumor agents and antibiotics is related to their mode of interaction with DNA, where groove binding and intercalation are known to be important. Structure–function relationship studies have been performed for intercalating drugs (1–4). The important features for intercalation have been suggested to be a fused tricyclic aromatic backbone and the presence of up to two flexible cationic side chains (1,3,5,6). The kinetics of guest binding to DNA has been investigated using stopped-flow techniques (2,4,7–17), surface plasmon resonance (18), pressure-jump measurements (19) and temperature jump studies (8,20,21). Relaxation processes were observed that span the millisecond to second time domain, and the kinetics were, in most cases, fitted to several exponential decays. Despite the suggestion that the duration of the dissociation process is important in determining the anticancer activity of intercalating molecules (2,5,10,11), there are only a few systematic studies on how the structure of

intercalating guests affects their association and dissociation rate constants with DNA.

The study of the host–guest binding dynamics is frequently limited experimentally when the dynamics are faster than the millisecond timescale accessible by stopped-flow or nuclear magnetic resonance (NMR) studies. Shorter timescales require photophysical methods where excited states are used to probe the mobility between the homogenous phase and the binding site inside the host (22–24). Excited singlet states of organic molecules are in general short-lived, and they do not relocate from their binding site. For this reason, fluorescence is used to gain information on the properties of the binding environment. In contrast, triplet excited states have long lifetimes and their dynamics between the homogenous phase and the binding site in the host can be measured either directly or with the use of quenchers located exclusively in the homogeneous phase (24).

Xanthone was chosen as the suitable chromophore for the present study because the mobility of its triplet state between environments of different polarity can be monitored directly (25–30). In addition, the xanthone backbone is found in a variety of compounds with potential biological action such as anti-inflammatory, antithrombotic, antimalarial, antibacterial and antitumor activities (31–37). In addition, xanthone has the tricyclic aromatic backbone necessary for intercalation with DNA. The triplet state of xanthone reacted with DNA (see below). For this reason, amino derivatives (Chart 1) of xanthone were synthesized with the expectation of lowering their photoreactivity toward DNA. We report on the photophysics of 2-aminoxanthone (MAX) and 2,7-diaminoxanthone (DAX) and explore the possibility of using these molecules to probe the binding dynamics with DNA.

MATERIALS AND METHODS

Synthesis: Instrumentation. Melting points were determined on a Gallenkamp (UK) melting point apparatus. Infrared spectra were recorded on a Perkin Elmer Spectrum 1000 FT-IR spectrometer (Vancouver, BC, Canada). Proton NMR spectra were recorded in CDCl₃ as solvent on a Bruker AC300 (300 MHz) spectrometer (Milton, ON, Canada). Mass spectra were recorded on a Finnigan 3300 gas chromatography–mass spectroscopy system (San Jose, CA) using methane gas for chemical ionization. The aminoxanthenes were tested for purity using a HP Series 1100 HPLC (Waldbronn, Germany) with spectrograde methanol as the eluent.

2-Nitroxanthone. Nitration was carried out following standard aromatic nitration procedures (38,39). A solution of KNO₃ (1.25 g, 12.3 mmol) in concentrated sulfuric acid (50 mL) was added slowly to a solution of xanthone (4.03 g, 20.6 mmol) in concentrated sulfuric acid (90 mL). The reaction mixture was allowed to stir at 20°C for 30 min and then the mixture was placed in an ice bath and slowly diluted with water (*T* ≤ 50°C). The pale yellow solid was isolated via vacuum filtration and recrystallized from

* To whom correspondence should be addressed: Department of Chemistry, University of Victoria, P.O. Box 3065, Victoria, BC V8W 3V6, Canada. Fax: 250-721-7147; e-mail: bohne@uvic.ca

[†] This paper is part of a special issue dedicated to Professor J. C. (Tito) Scaiano on the occasion of his 60th birthday.

Abbreviations: DAX, 2,7-diaminoxanthone; HPLC, high-performance liquid chromatography; MAX, 2-aminoxanthone; NMR, nuclear magnetic resonance.

© 2006 American Society for Photobiology 0031-8655/06

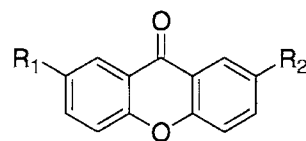
cold acetone and water, yielding 1.46 g (49%) of product, mp 198–200°C (literature values: 202.5°C [32], 200–204°C [39]). ¹H NMR (300 MHz) δ (CDCl₃) 9.21 (d, *J* = 2.9 Hz; 1H), 8.55 (dd, *J* = 8.8 Hz, 2.9 Hz; 1H), 8.35 (dd, *J* = 7.4 Hz, 1.5 Hz; 1H), 7.83–7.77 (m; 1H), 7.64 (d, *J* = 9.5 Hz; 1H), 7.55 (d, *J* = 8.0 Hz; 1H), 7.50–7.44 (m; 1H).

MAX. Reduction of nitro to amino groups was carried out following known procedures (39,40). A solution of stannous chloride (5.37 g, 28.3 mmol) in concentrated HCl (25 mL) was added dropwise to a solution of 2-nitroxanthone (1.05 g, 4.35 mmol) in concentrated HCl (125 mL). The reaction mixture was refluxed at 90–100°C for 2 h under nitrogen. The reaction was cooled to room temperature and excess potassium hydroxide (200 g in 400 mL water) was added. The bright yellow solid was isolated via vacuum filtration and then dissolved in CH₂Cl₂ and extracted with 2 N HCl (3 × 100 mL). The solution was basified with 10% NH₄OH and extracted with CH₂Cl₂ (3 × 100 mL). The organic phase was dried over anhydrous magnesium sulfate and the solvent was evaporated. The product was subjected to column chromatography (silica gel, 1:1 CH₃CN:CH₂Cl₂) and then dissolved in 99.99% 2 N HCl and precipitated with 99.99% 3 N NH₄OH, which gave 0.3 g (30%) as a yellow solid, mp 211–213°C (literature value: 210–212°C [40]). ¹H NMR (300 MHz) δ (CDCl₃) 8.26 (dd, *J* = 8.1 Hz, 2.2 Hz; 1H), 7.66–7.60 (m; 1H), 7.48 (d, *J* = 2.9 Hz; 1H), 7.39 (d, *J* = 8.1 Hz; 1H), 7.29 (d, *J* = 8.8 Hz; 1H), 7.27 (d, *J* = 8.1 Hz; 1H), 7.05 (dd, *J* = 8.8 Hz, 2.9 Hz; 1H); IR: 3685, 3055, 3047, 2986, 1651, 1627, 1608, 1492, 1468, 1329 cm⁻¹; CI MS *m/z* 240 (M+29), 213 (M+2), 212 (M+1), 211 (M⁺). The purity was checked by high-performance liquid chromatography (HPLC; 100% methanol, 25°C, 0.8 mL/min, monitored by absorption at 240, 250, 340, 350 and 500 nm) and by fluorescence (λ_{ex} = 340 nm, λ_{em} = 550 nm) and was found to be 100% pure at all detection wavelengths.

2,7-Dinitroxanthone. Nitration was carried out following standard aromatic nitration procedures (38,39). A solution of KNO₃ (2.34 g, 23.2 mmol) in concentrated sulfuric acid (100 mL) was added slowly to a solution of xanthone (1.52 g, 7.77 mmol) in concentrated sulfuric acid (20 mL). The reaction mixture was allowed to stir at 20°C for 2 h and then the mixture was placed in an ice bath and slowly diluted with water (*T* ≤ 50°C). The pale yellow solid was isolated via vacuum filtration and recrystallized from cold acetone and water, yielding 1.47 g (66%) of product, mp 261–263°C (literature values: 264°C [32], 262–265°C [39]). ¹H NMR (300 MHz) δ (CDCl₃) 9.22 (d, *J* = 2.9 Hz; 2H), 8.63 (dd, *J* = 9.2 Hz, 2.6 Hz; 2H), 7.72 (d, *J* = 9.6 Hz; 2H).

DAX. Reduction of nitro to amino groups was carried out following known procedures (39,40). A solution of stannous chloride (9.60 g, 50.6 mmol) in concentrated HCl (100 mL) was added dropwise to a solution of 2,7-dinitroxanthone (1.29 g, 4.50 mmol) in concentrated HCl (100 mL). The reaction mixture was refluxed at 90–100°C for 2 h under nitrogen. The reaction was cooled to room temperature and excess potassium hydroxide (200 g in 400 mL of water) was added. The bright yellow solid was isolated via vacuum filtration and then dissolved in CH₂Cl₂ and extracted with 2 N HCl (3 × 100 mL). The solution was basified with 10% NH₄OH and extracted with CH₂Cl₂ (3 × 100 mL). The organic phase was dried over anhydrous magnesium sulfate and the solvent was evaporated. The product was subjected to column chromatography (silica gel, 1:1 CH₃CN:CH₂Cl₂) and then dissolved in 99.99% 2 N HCl and precipitated with 99.99% 3 N NH₄OH, which gave 0.23 g (30%) as a yellow solid, mp 269–271°C (literature value: 272°C [39]). ¹H NMR (300 MHz) δ (CDCl₃) 7.50 (d, *J* = 2.9 Hz, 2H), 7.30 (d, *J* = 9.5 Hz; 2H), 7.07 (dd, *J* = 8.9 Hz, 3.0 Hz; 2H); IR: 3685, 2992, 2983, 1728, 1627, 1482, 1422, 1326 cm⁻¹; CI MS *m/z* 255 (M+29), 227 (M+1), 226 (M⁺). The purity was checked by HPLC (100% methanol, 25°C, 0.8 mL/min, monitored by absorption at 275, 350, 425, and 500 nm) and by fluorescence (λ_{ex} = 350 nm, λ_{em} = 500 nm) and was found to be 100% pure at all detection wavelengths.

Photophysical studies: Materials. Anthracene (99+%, Aldrich, Oakville, ON, Canada), naphthalene (99+%, scintillation grade, Aldrich), DNA (from calf thymus, Aldrich), guanosine (ICN Biomedicals, Aurora, OH), potassium phosphate dibasic (Caledon, Georgetown, ON, Canada) and potassium phosphate monobasic (BDH Chemicals, Toronto, ON, Canada) were used as received. Ferrocene (98%, Aldrich) was recrystallized and sublimed, 1,3-cyclohexadiene (97%, Aldrich) was distilled and sodium nitrite (97+%, Aldrich) was recrystallized from water before use. Deionized water (Sybron-Barnstead system) was used for all aqueous samples. Ethanol (95%, Commercial Alcohols, Brampton, ON, Canada), acetonitrile-190 (HPLC grade, Caledon) and cyclohexane (spectrograde, Caledon) were used as received.



R₁, R₂ = H Xanthone
 R₁ = H, R₂ = NH₂ 2-aminoxanthone (MAX)
 R₁, R₂ = NH₂ 2,7-diaminoxanthone (DAX)

Chart 1.

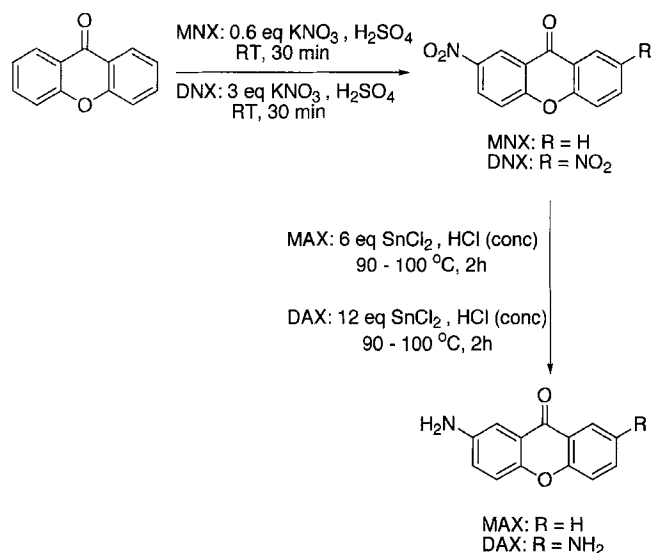
Instrumentation. Ground-state absorption spectra were measured on a Cary 1 Varian spectrophotometer (Mississauga, ON, Canada). Steady-state fluorescence spectra were obtained at constant temperature (20.0°C ± 0.2°C) using a PTI QM-2 fluorimeter (London, ON, Canada). The excitation and emission slits were set to optimize emission intensity, typically with a bandpass of 3 nm. The fluorescence spectra were corrected for the baseline spectrum of a solution containing all compounds except the aminoxanthones, ensuring that artifacts, such as Raman emission of the solvent, were subtracted from the fluorescence spectra. Time-resolved fluorescence measurements were performed with an OB-920 Edinburgh Instruments time-correlated single-photon counter (Livingston, UK). The slits were set to minimize the collection time, while keeping the frequency of stop pulses below 2% of the start pulse frequency. The number of counts in the channel of maximum intensity was 10 000. The instrument response function was measured using Ludox (Aldrich) as a scattering solution. Fitting of the fluorescence decays, where the instrument response function was deconvoluted from the experimental data, was performed using the Edinburgh software. The data were fitted to monoexponential decays. The value of χ² (0.9 to 1.3), the Durbin–Watson parameter (>1.7) (41) and a visual inspection of the residuals and the autocorrelation function were used to determine the quality of the fit. The laser flash photolysis system used for transient absorption measurements was described previously (29). MAX and DAX were excited at 308 nm with an Excimer laser from Lumonics (EX-510, Ottawa, ON, Canada) or at 355 nm using a Spectra Physics GCR-12 Nd:YAG laser (Mississauga, ON, Canada). Transient decays and transient spectra were measured using a Xe-arc lamp as the monitoring beam. Ten kinetic traces were averaged for each measurement. Experiments were performed at 20°C ± 2°C.

Sample preparation. All nonaqueous solutions were prepared by dissolving MAX or DAX such that, for fluorescence experiments, the absorbance of the sample at the excitation wavelength was lower than 0.1 in a 10 mm × 10 mm cell and, for laser flash photolysis experiments, the absorbance of the sample at the wavelength of irradiation was in the range of 0.1–0.3 in a 7 mm × 7 mm cell. Aqueous solutions of MAX or DAX were prepared by injecting small amounts of a methanolic stock solution (10 mM) into water or DNA aqueous solutions. The latter solutions were prepared by dissolving the appropriate amount of DNA in water or buffer solutions. The concentration of the aminoxanthones was approximately 20 μM for fluorescence experiments and 100 μM for laser flash photolysis experiments.

Deoxygenation procedures. Solutions for single photon counting experiments in nonaqueous media were deoxygenated by bubbling nitrogen for at least 20 min before use. All samples for laser flash photolysis measurements were deoxygenated by bubbling either nitrogen or nitrous oxide for at least 20 min before use.

Quenching methodology. For quenching experiments fresh quencher solutions were prepared daily. Stock solutions of 0.5 and 1 M 1,3-cyclohexadiene in cyclohexane, ethanol or acetonitrile, 0.5 M ferrocene in ethanol or acetonitrile and 1 M NaNO₂ in water were used. All quencher solutions were deoxygenated by bubbling nitrogen or nitrous oxide through them for at least 20 min before use. The appropriate volumes of quencher were added to 2-mL aliquots of the aminoxanthone solutions using a gas-tight syringe. For quenching experiments with guanosine, the guanosine (4 mM) was dissolved in 1:1 ethanol:water mixtures and MAX or DAX was added to this solution by injection of a methanolic stock solution of the xanthones.

Fluorescence quantum yield determination. Anthracene (φ_s = 0.27) or naphthalene (φ_s = 0.17) in ethanol was used as a standard with known fluorescence quantum yield (42). The fluorescence intensities for the standard (I_s) and sample with unknown quantum yield (I_u) were measured



Scheme 1.

for the same experimental conditions (*i.e.* constant emission and excitation slits) and the fluorescence quantum yield of the unknown in water (ϕ_f) was calculated using Eq. 1 (43):

$$\phi_f = \phi_s \frac{A_s J_u (n_u)^2}{A_u J_s (n_s)^2} \quad (1)$$

The absorbencies for the standard (A_s) and the unknown (A_u) were kept below 0.1 at the excitation wavelengths and were matched within ± 0.01 absorbance units for each individual experiment. The emission quantum yields were corrected for differences in the refractive indices (n) in different solvents. In each experiment the solutions for the standard and unknown were diluted to three different concentrations. The ϕ_f values for all concentrations were averaged. This procedure ensures the absence of systematic deviations due to aggregation of MAX and DAX at the higher concentrations of these compounds. At least two independent experiments were performed for the determination of each quantum yield value. The fluorescence quantum yield for anthracene and naphthalene are much higher than for MAX and DAX. For this reason, the emission for solutions containing the standards saturated the detector at settings of the fluorimeter where the emission of MAX and DAX could be measured. Instead of changing the bandwidth for the emission and excitation slits, which would lead to irreproducible results, we chose to use neutral density filters to attenuate the emission of anthracene and naphthalene. Emission spectra for these standard compounds were obtained in the absence and presence of neutral density filters and the appropriate corrections were made to the value of I_s used in Eq. 1.

Binding isotherms. The sample at the highest DNA concentration (< 4 mM with respect to base pair concentration) was prepared by the injection of small amounts of the methanolic MAX or DAX stock solutions into a DNA/buffer (10 mM phosphate buffer, pH 7) solution. This initial solution was diluted with a MAX or DAX/buffer solution containing the same concentration of the fluorophore as the initial solution to achieve lower DNA concentrations. The concentration of DNA was determined by UV spectroscopy ($\epsilon_{260} = 6500 \pm 100 \text{ M}^{-1} \text{ cm}^{-1}$ with respect to phosphate group concentration [21]). The fluorescence spectra at each DNA concentration were integrated and the binding was analyzed using the data treatment by McGhee and von Hippel (44). This model assumes that DNA consists of identical, noninteracting binding sites where the ligand occupies n base pairs and as binding approaches saturation the probability of finding a stretch of n unoccupied DNA base pairs decreases.

$$\frac{r}{L_{\text{free}}} = K(1 - nr) \left[\frac{1 - nr}{1 - (n-1)r} \right]^{n-1} \quad (2)$$

Where r is the ratio between concentration of bound MAX or DAX (L_{bound}) and the concentration of DNA base pairs, L_{free} is the concentration of MAX or DAX free in the aqueous phase and K is the equilibrium constant.

The parameter L_{bound} was evaluated from the fluorescence intensity values (A) at various DNA concentrations, where A_0 is the integrated area for the fluorescence in the absence of DNA and A_{max} is the extrapolated area when all MAX (DAX) was bound to DNA:

$$L_{\text{bound}} = [\text{MAX}] \left(\frac{A - A_0}{A_{\text{max}} - A_0} \right) \quad (3)$$

where $L_{\text{bound}} + L_{\text{free}} = [\text{MAX}]$.

RESULTS

Syntheses of aminoxanthenes

The synthesis of MAX and DAX was achieved by standard nitration of xanthone (38,39), followed by reduction of the nitro groups to amino moieties (39,40) (Scheme 1). The degree of nitration was controlled by optimizing the KNO₃/xanthone concentration ratio. For the synthesis of 2-nitroxanthone it was found that the order of addition of reagents was critical in obtaining selective mononitration. Both xanthone and potassium nitrate were dissolved separately in a minimum amount of concentrated sulfuric acid. When the xanthone solution was added to the nitrate solution a mixture of 2-nitroxanthone and 2,7-dinitroxanthone was obtained. When the addition was reversed the reaction yielded mostly 2-nitroxanthone. In addition, an excess of xanthone was used since the separation of 2-nitroxanthone from xanthone was easier than the separation of the desired product from 2,7-dinitroxanthone. The synthesis of 2,7-dinitroxanthone was carried out in the presence of excess potassium nitrate and the order of reagent addition did not matter. With the addition of excess nitrate the 2 and 7 positions are nitrated at room temperature, whereas further nitration at the 4 and 5 positions requires heating. Reduction of the nitrated xanthenes was carried out using stannous chloride as a reducing agent in concentrated hydrochloric acid. An excess of stannous chloride was used to ensure complete reduction of the nitro group. The products (MAX or DAX) were separated by column chromatography and were dissolved in HCl, followed by precipitation with NaOH. The purity of the amino xanthenes was checked by HPLC.

Photophysics of MAX and DAX

Fluorescence. The fluorescence emission spectra in water for MAX ($\lambda_{\text{max}} = 590 \pm 5$ nm) and DAX ($\lambda_{\text{max}} = 592 \pm 4$ nm) were significantly red-shifted when compared to the maximum for the emission spectrum of xanthone in water (396 nm) (26,45,46). The fluorescence maxima for MAX and DAX showed a marked dependence on solvent polarity, where a red shift was observed for polar solvents (Fig. 1), indicating that the singlet excited-state energy decreased as the solvent polarity increased. The absorption spectra in all solvents showed an absorption band centered around 370–390 nm. The shape of this absorption band did not change significantly in the different solvents. The absorption maximum for the longest wavelength band of MAX varied from 371 nm in cyclohexane to 389 nm in ethanol. Because of the significant Stokes shift between the absorption and emission spectra, the energy of the singlet excited state was calculated by averaging the wavelengths for the absorption maximum and the maximum of the fluorescence spectra. The energies for the first singlet excited state of MAX were determined to be 305 kJ/mol in cyclohexane, 286 kJ/mol in toluene, 268 kJ/mol in acetonitrile, 251 kJ/mol in ethanol and 247 kJ/mol in water. The singlet excited-state energy

for DAX in water was determined to be 241 kJ/mol. The same values were obtained within 5 kJ/mol for the singlet excited-state energies when these values were calculated from the intersection point of the normalized absorption and fluorescence spectra. This latter method could not be used for the spectra in water because of the large separation of the spectra and the poor signal-to-noise ratio at the intersection point. The singlet excited-state energies for MAX and DAX are much lower than the singlet excited-state energies for xanthone, which vary from 334 kJ/mol in hexane to 329 kJ/mol in acetonitrile (47).

The fluorescence quantum yields for xanthone, MAX and DAX were measured in water. The measured fluorescence quantum yield for MAX ($[0.9 \pm 0.1] \times 10^{-3}$) and DAX ($[1.0 \pm 0.1] \times 10^{-3}$) were much lower than the quantum yield determined for xanthone ($[17 \pm 2] \times 10^{-3}$). The relative emission intensities in different solvents were estimated by integrating the fluorescence spectra and taking into account the fraction of absorbed photons ($1-10^{-A}$, where A is the absorbance) for solutions with different absorbance values at the excitation wavelength. The relative emission intensities for MAX were 1 in water, 9 in ethanol, 130 in acetonitrile and 210 in toluene, showing that the fluorescence quantum yield is very dependent on the nature of the solvent. The relative intensities only provide estimates for quantum yields since samples were used with variable absorbance at the excitation wavelength ($A = 0.01-0.06$) because of the low solubility of MAX and the very different emission efficiencies. It is important to note that MAX and DAX are not completely solubilized even at relatively low concentrations (*ca* 50 μM), leading to the appearance of shoulders in the fluorescence spectra at shorter wavelengths in water and longer wavelengths in cyclohexane and toluene. Such an effect was previously reported (48); however, the assignment of the emission bands was different from ours. This discrepancy is likely due to sample preparation, but could not be further pursued because of the lack of details in the previous report.

The lifetimes for the decay of the singlet excited states of MAX and DAX in acetonitrile were 22.3 ± 0.3 ns and 17.5 ± 0.1 ns, respectively. In water the decay profile for the MAX and DAX fluorescence was very close to the profile for the instrument response function, indicating that the lifetimes of MAX and DAX in water are shorter than 1 ns. This result is consistent with the large changes observed for the fluorescence efficiency in the steady-state spectra. The singlet excited-state lifetime of MAX was estimated from quenching experiments in acetonitrile/water mixtures. Addition of water to MAX in acetonitrile led to a decrease of the emission intensity and a red shift of the maximum for the fluorescence spectra. The ratio of the integrated area of the fluorescence spectra in the absence (A_0) and presence (A) of water varied linearly with the water concentration up to a concentration of 10 M. The product of the quenching rate constant and the lifetime in the absence of water ($k_q\tau_0$, Eq. 4) was $1.9 \pm 0.1 \text{ M}^{-1}$, leading to a quenching rate constant by water of $(8.5 \pm 0.5) \times 10^7 \text{ M}^{-1} \text{ s}^{-1}$. The lifetime for the singlet excited state of MAX was estimated to be *ca* 0.2 ns by assuming that the linear relation held for high water concentrations.

$$\frac{A_0}{A} = 1 + k_q\tau_0 [\text{water}] \quad (4)$$

Transient spectroscopy. MAX and DAX were excited either at 308 or 355 nm. The transient kinetics observed were independent of the laser excitation wavelength. In polar solvents, such as

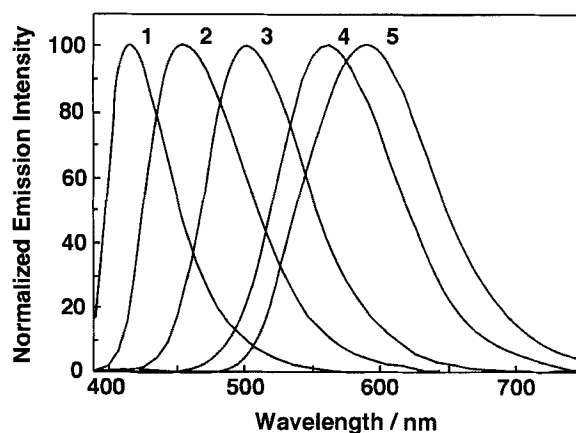


Figure 1. Normalized fluorescence spectra of MAX in cyclohexane (1), toluene (2), acetonitrile (3), ethanol (4) and water (5). The excitation wavelength was 380 nm and the MAX concentrations were varied between 2 and 10 μM .

acetonitrile, ethanol and water, the absorption for solvated electrons was detected above 600 nm. This observation indicates that MAX and DAX are photoionized, a reaction commonly seen for ketones and aromatic hydrocarbons in polar solutions in the absence and presence of host systems (49–51). The occurrence of this process can be attenuated by decreasing the laser pulse energy because, in most cases, photoionization involves the sequential absorption of two photons. Solutions were also bubbled with N_2O , a known trap for solvated electrons (52).

In cyclohexane a transient absorption for MAX with a maximum around 600 nm was observed, which was assigned to the triplet excited state (see below), while bleaching of the precursor was seen in the 350 to 400 nm region (Fig. 2a). At long delays a residual absorption with a maximum at 440 nm was observed. In polar nonprotic solvents such as acetonitrile (Fig. 2a), the transient spectrum for MAX broadens. In phosphate buffer the transient absorption maximum for MAX was shifted to 440–460 nm (Fig. 2b). The same shift was observed for the spectrum in ethanol. The signals were much weaker in ethanol or cyclohexane for solutions with equivalent absorptions at the excitation wavelength. The transient absorption spectra for DAX had similar features to those observed for MAX, with the whole absorption spectrum being red-shifted, *e.g.* the maximum in water was observed around 530 nm. The decays were measured at the transient absorption maxima and the kinetics followed a monoexponential decay for MAX and DAX in cyclohexane, acetonitrile and ethanol. The lifetimes were in excess of 5 μs , with the exception of cyclohexane where the lifetime was 0.6 μs . In the case of water, a small component with a short lifetime was observed. The predominant component of the kinetics was long-lived, with a lifetime in excess of 60 μs . The transient spectra for the fast component were similar to the spectra for the long-lived component. The fast component was assigned to the decay of the transient in aggregated MAX and DAX formed at the concentrations used for laser flash photolysis studies where these compounds may not be completely solubilized. Unfortunately, dilute solutions could not be studied in the laser flash photolysis experiments because of the weak signals observed.

Quenching and sensitization experiments were performed to assign the transients observed in the laser flash photolysis experiments. The quenching rate constants (k_q) were obtained from the

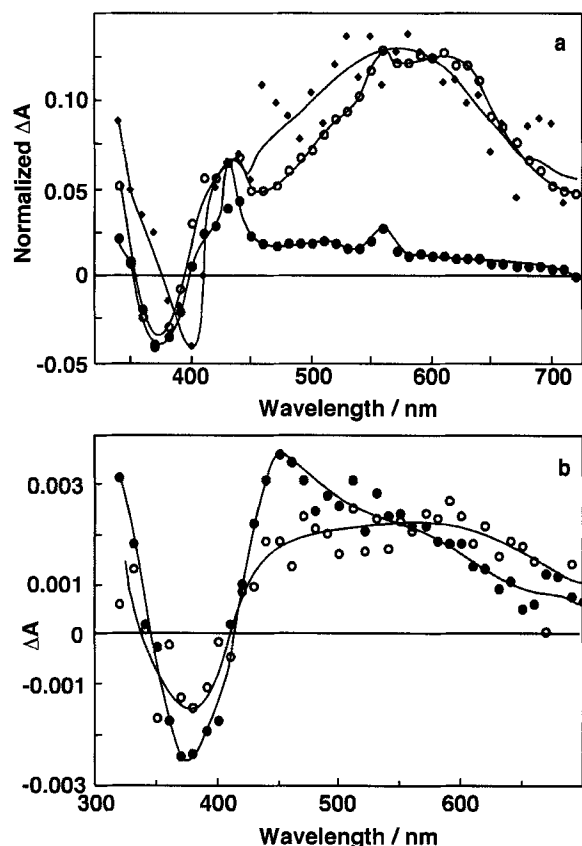


Figure 2. (a) Transient absorption spectra for MAX in cyclohexane at delays after the laser pulse of 240 ns (\circ) and 6.4 μ s (\bullet) and MAX in acetonitrile (\blacklozenge , 830 ns delay). The spectrum in acetonitrile was normalized at 600 nm to the spectrum in cyclohexane. (b) Transient absorption spectra of MAX in 10 mM phosphate buffer (pH 7.0) in the absence (\bullet , 10 μ s delay) and presence (\circ , 10 μ s delay) of 4 mM calf thymus DNA.

dependence of the observed rate constant (k_{obs}) with the quencher concentration (Eq. 5):

$$k_{\text{obs}} = k_0 + k_q [\text{quencher}] \quad (5)$$

The decays were measured at the transient's absorption maximum. In all solvents the transients were efficiently quenched by

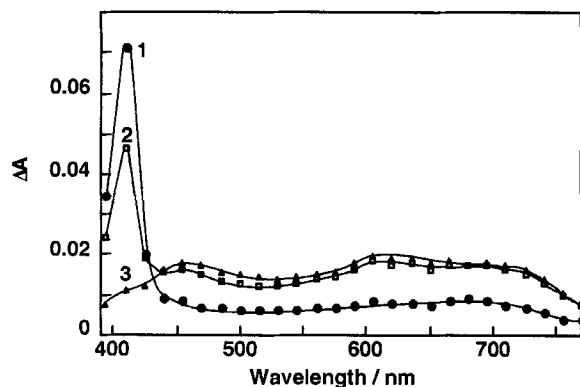


Figure 3. Transient absorption spectra of DAX in the presence of naphthalene in 1:1 acetonitrile:water at delays of 290 ns (1), 1 μ s (2) and 4.4 μ s (3) after the laser pulse. The sharp absorption around 420 nm corresponds to the absorption for triplet naphthalene and the broad absorption centered around 600 nm corresponds to triplet DAX.

Table 1. Quenching rate constants for the triplet states of MAX and DAX by 1,3-cyclohexadiene and ferrocene in various solvents.

Solvent	$k_q/10^8 \text{ M}^{-1} \text{ s}^{-1}$			
	MAX		DAX	
	1,3-Cyclohexadiene	Ferrocene	1,3-Cyclohexadiene	Ferrocene
Cyclohexane	55 ± 3	*	*	*
Acetonitrile	2.4 ± 0.6	11 ± 2	2.7 ± 0.5	11 ± 1
Ethanol	0.0056 ± 0.0002	25 ± 7	<0.001	2.7 ± 0.1

* Not measured.

oxygen in a diffusion-controlled process. For example, the k_q values for the quenching of the transients of MAX and DAX in ethanol were $(2.3 \pm 0.1) \times 10^9 \text{ M}^{-1} \text{ s}^{-1}$ and $(3.3 \pm 0.1) \times 10^9 \text{ M}^{-1} \text{ s}^{-1}$, respectively. Quenching of triplet excited states by 1,3-cyclohexadiene occurs through energy transfer, where the triplet energy of the quencher is 218 kJ/mol (53). In contrast, 1,4-cyclohexadiene quenches triplet states through hydrogen atom transfer. The transient for MAX in cyclohexane was quenched by 1,3-cyclohexadiene, but no quenching was observed for 1,4-cyclohexadiene. This quenching pattern is consistent with the formation of a triplet excited state that cannot undergo hydrogen abstraction reactions, indicating that the configuration of the excited state is π, π^* .

A very significant solvent effect was observed on the quenching efficiency of the transient by 1,3-cyclohexadiene (Table 1). This result showed that the energy for the triplet excited state decreased as the polarity of the solvent was raised. In cyclohexane the k_q value is close to the rate constant for a diffusional controlled process ($6.7 \times 10^9 \text{ M}^{-1} \text{ s}^{-1}$) (53), whereas in acetonitrile the value for the quenching rate constant is more than one order of magnitude smaller than the diffusional controlled limit and in ethanol the quenching rate constant decreases by several orders of magnitude. Ferrocene was used as a quencher with a lower triplet energy (159 kJ/mol) (53). In this case the rate constants were much higher than for the quenching with the diene (Table 1).

The lower quenching rate constants observed in ethanol could result from the formation of a transient different from the triplet excited state of MAX and DAX. Sensitization experiments were performed to confirm that the transients in protic solvents were the triplet excited states of these compounds. A 1:1 acetonitrile:water mixture was used to enhance the solubility of the organic compounds. Naphthalene was used as a triplet sensitizer and was excited at 308 nm. The triplet state of naphthalene has a sharp absorption at 420 nm (54). The lifetime of triplet naphthalene was measured from the kinetics at 420 nm and it was shortened with the addition of MAX or DAX. The quenching rate constant was estimated from the lifetimes measured in the absence of MAX or DAX and at one concentration of these xanthone derivatives. The estimated quenching rate constant was higher than $5 \times 10^9 \text{ M}^{-1} \text{ s}^{-1}$. Transient spectra of a naphthalene/DAX aqueous solution showed the sharp absorption due to the triplet naphthalene at short delays after the laser pulse, whereas at long delays, when quenching of the triplet naphthalene had occurred, a broad spectrum was observed (Fig. 3). This spectrum is similar to that observed for the direct excitation of DAX in water. These results clearly show that the transient observed in protic solvents is the triplet excited state of MAX and DAX.

Several quenching experiments were performed that were relevant for studying the dynamics of MAX and DAX binding to DNA. One requirement for these studies is that the triplet state be formed for the bound guest (MAX or DAX) and that the excited guests not react with the host (DNA). For this reason, the quenching of triplet MAX by guanosine was investigated in a 1:1 ethanol:water solution. No quenching was observed for a guanosine concentration as high as 4 mM. The highest guanosine concentration used was limited by the solubility of this compound in ethanol/water (1:1). Nitrite is frequently used as the quencher when applying the quenching methodology (see below) to determine the association and dissociation rate constants of guests with hosts. Nitrite ions efficiently quench triplet states through an energy transfer process (55). Triplet MAX in buffer solutions (10 mM phosphate buffer, pH = 7.0) was quenched by nitrite ions with a rate constant of $(2.2 \pm 0.2) \times 10^6 \text{ M}^{-1} \text{ s}^{-1}$. The quenching efficiency for the triplet state of DAX by nitrite is at least one order of magnitude lower than observed for MAX. These values are much lower than the values between 2×10^9 and $6 \times 10^9 \text{ M}^{-1} \text{ s}^{-1}$ observed for the quenching of triplet naphthalenes and triplet ketones, such as benzophenone and xanthone (56–59).

MAX and DAX binding to DNA

Addition of DNA to buffered aqueous solutions containing MAX or DAX led to an increase in the fluorescence intensity and a blue shift of the emission maximum to 545–550 nm (Fig. 4). This result showed that MAX and DAX were bound to DNA, and that the binding site is slightly less polar than water. The position of the fluorescence maximum in the presence of DNA is intermediate to the emission maxima observed for MAX in acetonitrile (505 nm) and ethanol (562 nm). The decay for the MAX and DAX fluorescence in the presence of DNA could not be deconvoluted from the instrument response function in the single photon counting experiment. The increase of the fluorescence intensity in the steady-state experiments suggests that the lifetimes of MAX and DAX increased when these compounds were bound to DNA. However, the increase from the estimated lifetime in water of 0.2 ns was small enough that the lifetimes of MAX and DAX bound to DNA were shorter than 1 ns.

In the presence of DNA the integrated area for the fluorescence of MAX or DAX corresponds to the sum of the emission of MAX (DAX) free in the aqueous solution and the fluorophore bound to DNA, taking into account the relative concentrations of the bound and free species. An analysis assuming noninteracting and identical sites (44) was used to estimate the equilibrium constants for MAX or DAX binding to DNA (inset Fig. 4). The analysis requires the emission intensity to be known when all the guests are bound to DNA (A_{max}). Unfortunately a complete saturation of the emission intensity with an increase of the DNA concentration was not achievable. The value of A_{max} was estimated by fitting the variation of the change in fluorescence intensity (ΔA) with DNA concentration to a hyperbolic function, where A_{max} is the extrapolated asymptotic value at high DNA concentration. The recovered values for K were $(6.6 \pm 0.5) \times 10^3 \text{ M}^{-1}$ for MAX and $(3.8 \pm 0.1) \times 10^3 \text{ M}^{-1}$ for DAX, whereas the number of base pairs per binding site was 9 ± 1 for MAX and 12 ± 1 for DAX. The n values are too large for the binding of a small molecule to DNA. This is probably due to the uncertainty of the data at high r values that leads to the inaccuracy in the n value. The parameter $1/n$ is the intercept of the plot with the x -axis and data points at larger r values would be

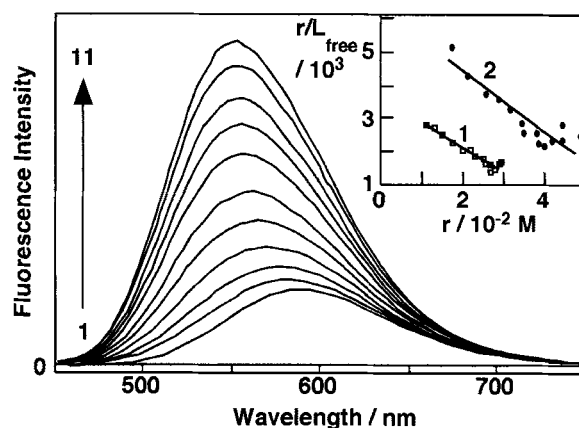


Figure 4. DAX (10 μM) fluorescence emission in 10 mM phosphate buffer (pH 7.0) in the presence of increasing concentrations of calf thymus DNA (mM), 1: 0; 2: 0.018; 3: 0.074; 4: 0.28; 5: 0.46; 6: 0.65; 7: 1.0; 8: 1.4; 9: 1.8; 10: 2.8; 11: 3.7. Inset: McGhee–von Hippel plots for the binding of DAX (\square , 1) and MAX (\bullet , 2) to calf thymus DNA.

required to decrease the inaccuracy in n . Unfortunately these values of r could not be achieved for the MAX/DNA system.

The lifetimes for the singlet excited states of MAX and DAX are too short for these species to relocate during the excited-state lifetime between the binding site in DNA and the aqueous phase. Triplet excited states are much longer lived and are, therefore, suitable to measure the binding dynamics between guests and hosts (24). The association (k_+) and dissociation rate constants (k_-) between the guest and host can be obtained by using a quencher that primarily resides in the aqueous phase (24,56,59–61). Conceptually, as the quencher concentration increases in the aqueous phase the host acts as a reservoir for triplet states, slowing down the quenching process when compared to this reaction in the aqueous phase. This slowdown leads to a nonlinear relation between the observed rate constant (k_{obs}) and quencher concentration expressed by equation (6):

$$k_{\text{obs}} = \frac{k_{\text{DNA}} + k_- + k_q^{\text{DNA}} [\text{nitrite}]}{k_0 + k_q [\text{nitrite}] + k_+ [\text{DNA binding sites}]} \quad (6)$$

where k_0 and k_{DNA} are the lifetimes of the triplet excited states in water and within the DNA, and k_q and k_q^{DNA} are the quenching rate constants for triplet MAX or DAX by nitrite in water and for the DNA-bound guests.

The triplet-triplet absorption spectra for MAX (Fig. 2b) and DAX in the presence of DNA are broad and featureless, as are the transient spectra observed for these compounds in water. The smaller transient absorption for MAX in the presence of DNA in the 450 nm region is due to a slight broadening and red shift of the MAX ground-state absorption spectrum in this spectral region. This change led to a decrease in the transient absorption because it corresponds to the difference between the absorption of the transient and the ground state.

The quenching plot for MAX in the presence of DNA was linear and the quenching efficiency was much lower than observed for the quenching of triplet MAX in water (Fig. 5). Unfortunately, higher nitrite concentrations could not be used because of a deterioration of the signal-to-noise level for the absorption of triplet MAX. The fact that the quenching plot does not curve in the presence of DNA

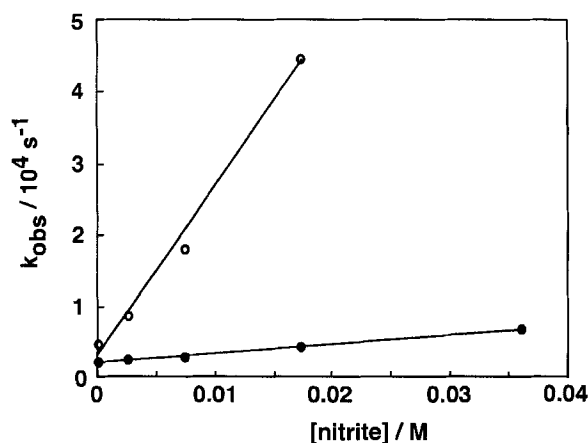


Figure 5. Nitrite quenching plot for the MAX triplet excited state in 10 mM phosphate buffer (pH 7.0) in the absence (○) and presence (●) of 1.4 mM calf thymus DNA.

precluded the determination of the values for k_+ and k_- . The slope of the quenching plot ($[1.3 \pm 0.2] \times 10^5 \text{ M}^{-1} \text{ s}^{-1}$) provides an upper limit for the value of k_q^{DNA} .

DISCUSSION

The binding dynamics of guests with DNA have previously been studied using stopped-flow techniques (2,4,7–17), surface plasmon resonance (18), pressure-jump measurements (19) and temperature jump studies (8,20,21). These studies established that the binding dynamics are complex, *i.e.* do not follow a monoexponential relaxation process. However, detailed mechanistic information on the significance of the various relaxation processes and the effect of structural changes to the guest and DNA has not been systematically investigated. This information will be required to establish to what extent dynamic events, such as the residence time of the guest within DNA, have an effect on biological function.

Laser flash photolysis experiments have been used to study the guest binding dynamics to host systems such as micelles, cyclodextrin and bile salt aggregates (24). In these investigations a long-lived transient, such as a triplet excited state, is formed by a laser pulse and its association and dissociation rate constants with the host are measured either directly or by using the quenching methodology (24). The requirements to apply laser flash photolysis to study the binding dynamics of guests to DNA are: (1) nonreactive singlet and triplet excited states of the guest, so that transients formed from reaction with DNA do not interfere with the study of the binding dynamics; (2) singlet and triplet excited-state energies that are lower than the excited-state energies of the DNA bases ($E_S = 400\text{--}420 \text{ kJ/mol}$; $E_T = 310\text{--}340 \text{ kJ/mol}$ [53]) to avoid deactivation of the excited states by energy transfer; (3) a long-lived triplet excited state so that the excited guest can move between the binding site in DNA and the aqueous phase. Our preliminary laser flash photolysis experiments with xanthone in the presence of DNA showed the formation of transient species different from the triplet excited state of the ketone, suggesting that the triplet state of xanthone was reacting with DNA. This reactivity was confirmed in a report where xanthone was shown to damage double-stranded DNA through an electron transfer mechanism (62). We reasoned that substitution of the xanthone chromophore with electron-donating substituents, such as amino groups, would reduce the photoreactivity of the excited states toward DNA.

The aminoxanthenes showed a marked solvatochromic effect on their photophysics when compared to xanthone. The singlet excited-state energies for MAX and DAX are significantly lower than observed for the singlet excited state of xanthone, and the excited-state energy decreased to a much greater extent in polar solvents for the amino-substituted xanthenes. The latter observation suggests that the lowest excited state has a significant charge transfer character in MAX and DAX. A similar effect was previously observed for amino-substituted aromatic ketones, such as fluorenones and anthraquinones (63,64). The charge transfer character of the first singlet excited state is also responsible for the shorter lifetimes observed in protic solvents, such as alcohols and water. The increase of the internal conversion rate constant of amino-substituted fluorenones and anthraquinones was previously assigned to the hydrogen bonding of the solvent to the carbonyl moiety of these compounds, leading to an effective deactivation channel for the excited state (63–67).

A solvatochromic effect was also observed for the triplet states of MAX and DAX. Quenching and sensitization experiments established that the transient observed in all solvents was the triplet state of the aminoxanthenes. A smaller absorbance was observed after the laser pulse for MAX and DAX in water when compared to other solvents, suggesting that the intersystem crossing yield in water was lower. This result is consistent with the shorter singlet excited-state lifetime observed in water (*ca* 0.2 ns) when compared to acetonitrile (17–22 ns). The triplet-triplet absorption spectra shifted to longer wavelengths and a broadening of the spectra was observed in solvents with hydrogen bonding ability. This result suggests that hydrogen bonding of the solvent to the fluorophore also occurs in the case of the triplet excited state, but in contrast to the singlet excited state it does not significantly decrease the triplet excited-state lifetime. For example, in water the triplet lifetime was in excess of 60 μs .

The solvent polarity has a very significant effect on the triplet excited-state energy. The quenching rate constants decreased as the polarity of the solvent was increased, suggesting a marked decrease of the triplet energies. This behavior is consistent with an excited state that has charge-transfer character, because as the solvent polarity is raised the excited state is stabilized with respect to the ground state. Analysis of the quenching rate constants gives an estimate of the triplet energies, provided quenching occurs through energy transfer, which is the case for 1,3-cyclohexadiene, ferrocene and the nitrite anion. When the triplet energy of the quencher is much lower than the triplet energy of the excited state, the value for the quenching rate constant is close to the diffusion-controlled limit, whereas a decrease of orders of magnitude is observed for the rate constant when the triplet energy of the quencher is higher than the energy of the excited state being quenched. The triplet energy for MAX decreased from a value higher than 218 kJ/mol in cyclohexane to a value close to 218 kJ/mol in acetonitrile. In ethanol the triplet energy is reduced further, but it is somewhat higher than the energy for triplet ferrocene (159 kJ/mol). The triplet energies for MAX and DAX are higher than the triplet energy of ferrocene in acetonitrile. However, the quenching rate constant by ferrocene in ethanol is one order of magnitude smaller for DAX than for MAX, suggesting that the energy for the triplet state is lower for DAX than for MAX. The lower triplet energy of DAX can be explained by a higher charge-transfer character of its excited state when compared to the excited state of MAX, since DAX contains two amino substituents. The triplet energies are also low in water since the quenching rate

constant by nitrite, which has a triplet energy of 222 kJ/mol (55), is at least three orders of magnitude smaller than the diffusional rate constant.

MAX and DAX form complexes with DNA with a reasonable binding affinity ($K \sim 3\text{--}7 \times 10^3 \text{ M}^{-1}$). The binding mode for MAX and DAX with DNA, *i.e.* intercalation or groove binding, was not established. The singlet excited-state lifetimes for MAX and DAX were shorter than 1 ns, suggesting that the lengthening of the lifetime due to binding to DNA was only modest. This result suggests that in the binding site of DNA there is some hydrogen bonding from DNA or the solvent to the carbonyl group of the ketones.

The association and dissociation rate constants of a guest with host systems is studied by following the kinetics of the triplet excited state of the guest, since its long lifetime ensures that it can relocate between the binding site and the aqueous phase. The triplet state lifetimes for MAX and DAX in the presence of DNA are equal to or longer than the lifetimes in water. No new transients were observed in the presence of DNA, confirming that the triplet states of MAX and DAX are nonreactive toward DNA. This result is consistent with the lack of quenching we observed for the triplet state of MAX by guanosine. There are two possible reasons for the decreased photoreactivity of MAX and DAX toward DNA when compared to the reactivity demonstrated by xanthone. The lower triplet energy could be insufficient to drive the electron transfer process or the electron-donating substituents could decrease the stability of the radical anion formed in an electron transfer process.

The long-lived triplet states of MAX and DAX observed in the presence of DNA correspond to excited states of the ketones bound to the DNA. This is demonstrated by the lower quenching efficiency by nitrite anions in the presence of DNA when compared to the quenching efficiency in water. Unfortunately the quenching plots in the presence of DNA were not curved, which precluded the determination of the association and dissociation rate constants of MAX and DAX with DNA. The limitation of the experiment is that higher nitrite concentrations could not be used because they degraded the signal-to-noise ratio because of absorption of the laser light by the quencher. Higher concentrations of nitrite anions, when compared to studies with other host-guest systems, were required for the quenching of triplet MAX and DAX because the quenching rate constants for these compounds in water were *ca* three orders of magnitude lower than observed for other excited-state guests. For this reason, we were unable to achieve the plateau region where the kinetics is limited by the exit of the excited-state guest from the host binding site. We can estimate the lowest possible value for k_{-} by assuming that the last point in the quenching plot is the lowest possible value for the observed rate constant at which the quenching plot could have leveled off. From this value we estimate that k_{-} has to be equal to or larger than $0.7 \times 10^4 \text{ s}^{-1}$ for MAX. The highest value for the dissociation rate constant can be estimated from the equilibrium constant since it is equal to the ratio of the association and dissociation rate constants ($K = k_{+}/k_{-}$). The highest k_{-} will occur when the association is diffusion controlled ($6.5 \times 10^9 \text{ M}^{-1} \text{ s}^{-1}$ at 20°C [53]), and is estimated to be *ca* $2 \times 10^6 \text{ s}^{-1}$. Therefore the residence time for MAX in DNA can be bracketed between 1.0 and 140 μs . This estimate shows that the residence time of MAX within DNA is short and exit occurs in the microsecond time domain. Since the binding mode of MAX with DNA was not determined we cannot comment if this fast dynamics corresponds to intercalation or a groove binding mode. Systematic studies on the binding

kinetics will only be possible when a kinetic technique is developed to achieve real-time kinetic studies in the microsecond time domain.

CONCLUSION

Substitution of xanthone with electron-donating amino groups led to the desired stabilization of these molecules with respect to their photoreactivity toward DNA, and we achieved the objective of identifying guest molecules where the triplet excited state is long-lived and unreactive when bound to DNA. Unfortunately the extent of the stabilization required led to a decrease of the triplet state energies, which made the quenching methodology unsuitable to determine the association and dissociation rate constants of MAX and DAX with DNA, and we could only estimate that the residence time of bound MAX was in the microsecond time domain. These results showed that the quenching methodology is not widely applicable to study the binding dynamics of guests with DNA since only a small number of molecules will simultaneously fulfill the requirement of not being photoreactive toward DNA and have a high enough triplet excited-state energy for the quenching methodology to be applicable.

Acknowledgements—The authors thank the Natural Sciences and Engineering Research Council of Canada (NSERC) for the financial support of this research, and L. Netter for support with software development. T.C.S.P. and A.I.M. thank the University of Victoria for their Graduate Scholarships.

REFERENCES

- Atwell, G. L., B. Cain, B. C. Baguley, G. L. Finlay and W. A. Denny (1984) Potential antitumor agents. 43. Synthesis and biological activity of dibasic 9-aminoacridine-4-carboxamides, a new class of antitumor agent. *J. Med. Chem.* **27**, 1481–1485.
- Denny, W. A., G. J. Atwell, B. C. Baguley and L. P. G. Wakelin (1985) Potential antitumor agents. 44. Synthesis and antitumor activity of new classes of diacridines: importance of linker chain rigidity for DNA binding kinetics and biological activity. *J. Med. Chem.* **28**, 1568–1574.
- Murdock, K. C., R. G. Child, Y.-I. Lin, J. D. Warren, P. F. Fabio, V. J. Lee, P. T. Izzo, S. A. J. Lang, R. B. Angier, R. V. Citarella, R. E. Wassace and F. E. Durr (1982) Antitumor agents. 2. Bisguanylhydrazones of anthracene-9,10-dicarboxaldehydes. *J. Med. Chem.* **25**, 505–518.
- Wakelin, L. P. G., G. J. Atwell, G. W. Rewcastle and W. A. Denny (1987) Relationships between DNA-binding kinetics and biological activity for the 9-aminoacridine-4-carboxamide class of antitumor agents. *J. Med. Chem.* **30**, 855–861.
- Feigon, J., W. A. Denny, W. Leupin and D. R. Kearns (1984) Interactions of antitumor drugs with natural DNA: 1H NMR study of binding mode and kinetics. *J. Med. Chem.* **27**, 450–465.
- Wakelin, L. P. G., P. Chetcuti and W. A. Denny (1990) Kinetic and equilibrium binding studies of acridine-4-carboxamides: a class of asymmetrical DNA-intercalating agents which bind by threading through the DNA helix. *J. Med. Chem.* **33**, 2039–2044.
- Adams, A., J. M. Guss, C. A. Collyer, W. A. Denny, A. S. Pradash and L. P. G. Wakelin (2000) Acridinecarboxamide topoisomerase poisons: structural and kinetic studies of the DNA complexes of 5-substituted 9-mino(-N-(2-dimethylamino)ethyl)acridine-4-carboxamides. *Mol. Pharm.* **58**, 649–658.
- Chaires, J. B., N. Dattagupta and D. M. Crothers (1985) Kinetics of the daunomycin-DNA interaction. *Biochemistry* **24**, 260–267.
- Fox, K. R., C. Brassett and M. J. Waring (1985) Kinetics of dissociation of nogalamycin from DNA: comparison with other anthracycline antibiotics. *Biochim. Biophys. Acta* **840**, 383–392.
- Fox, K. R., L. P. G. Wakelin and M. J. Waring (1981) Kinetics of the interaction between echinomycin and deoxyribonucleic acid. *Biochemistry* **20**, 5768–5779.

11. Gabbay, E. J., D. Grier, R. E. Fingerle, R. Reimer, R. Levy, S. W. Pearce and W. D. Wilson (1976) Interaction specificity of the anthracyclines with deoxyribonucleic acid. *Biochemistry* **15**, 2062–2070.
12. Müller, W. and D. M. Crothers (1968) Studies of binding of actinomycin and related compounds to DNA. *J. Mol. Biol.* **35**, 251–290.
13. Phillips, D. R., P. C. Greif and R. C. Boston (1988) Daunomycin-DNA dissociation kinetics. *Mol. Pharmacol.* **33**, 225–230.
14. Taniou, F. A., T. C. Jenkins, S. Neidle and W. D. Wilson (1992) Substituent position dictates the intercalative DNA-binding mode for anthracene-9,10-dione antitumor drugs. *Biochemistry* **31**, 11632–11640.
15. Taniou, F. A., D. Ding, D. A. Patrick, R. R. Tidwell and W. D. Wilson (1997) A new type of DNA minor-groove complex: carbazole dication-DNA interactions. *Biochemistry* **36**, 15315–15325.
16. Wakelin, L. P. G., A. Adams and W. A. Denny (2002) Kinetic studies of the binding of acridinecarboxamide topoisomerase poisons to DNA: implications for mode of binding of ligands with uncharged chromophores. *J. Med. Chem.* **45**, 894–901.
17. Westerlund, F., L. M. Wilhelmsson, B. Norden and P. Lincoln (2003) Micelle-sequestered dissociation of cationic DNA-intercalated drugs: unexpected surfactant-induced rate enhancement. *J. Am. Chem. Soc.* **125**, 3773–3779.
18. Lacy, E. R., N. M. Le, C. A. Price, M. Lee and W. D. Wilson (2002) Influence of a terminal formamido group on the sequence recognition of DNA by polyamides. *J. Am. Chem. Soc.* **124**, 2153–2163.
19. Marcandalli, B., W. Knoche and J. F. Holzwarth (1986) A pressure-jump investigation of the binding of proflavine to calf-thymus DNA. *Gaz. Chim. Ital.* **116**, 417–421.
20. Li, H. J. and D. M. Crothers (1969) Relaxation studies of the proflavine-DNA complex: the kinetics of an intercalation reaction. *J. Mol. Biol.* **39**, 461–477.
21. Marcandalli, B., C. Winzek and J. F. Holzwarth (1984) A laser temperature jump investigation of the interaction between proflavine and calf-thymus deoxyribonucleic acid at low and high ionic strength avoiding electric field effects. *Ber. Bunsenges. Phys. Chem.* **88**, 368–374.
22. Kalyanasundaram, K. (1987) *Photochemistry in Microheterogeneous Systems*, p. 388. Academic Press, Orlando.
23. Ramamurthy, V. (1991) *Photochemistry in Organized and Constrained Media*, p. 875. VCH Publishers, New York.
24. Kleinman, M. H. and C. Bohne (1997) Use of photophysical probes to study dynamic processes in supramolecular structures. In *Molecular and Supramolecular Photochemistry* (Edited by V. Ramamurthy and K. S. Schanze), pp.391–466. Marcel Dekker, New York.
25. Abuin, E. B. and J. C. Scaiano (1984) Exploratory study of the effect of polyelectrolyte-surfactant aggregates on photochemical behavior. *J. Am. Chem. Soc.* **106**, 6274–6283.
26. Barra, M., C. Bohne and J. C. Scaiano (1990) Effect of cyclodextrin complexation on the photochemistry of xanthone. Absolute measurement of the kinetics for triplet-state exit. *J. Am. Chem. Soc.* **112**, 8075–8079.
27. Liao, Y., J. Frank, J. F. Holzwarth and C. Bohne (1995) Effect of excitation on the host-guest equilibrium constants of cyclodextrin complexes. *J. Chem. Soc. Chem. Commun.* 199–200.
28. Liao, Y., J. Frank, J. F. Holzwarth and C. Bohne (1995) Comments on the interpretation of triplet excited-state decay data for the determination of the equilibrium constants in host-guest cyclodextrin complexes. *J. Chem. Soc. Chem. Commun.* 2435–2436.
29. Liao, Y. and C. Bohne (1996) Alcohol effect on equilibrium constants and dissociation dynamics of xanthone-cyclodextrin complexes. *J. Phys. Chem.* **100**, 734–743.
30. Barra, M. (1997) Deuterium isotope effect on the complexation of β -cyclodextrin and triplet xanthone in aqueous solution. *Supramolec. Chem.* **8**, 263–266.
31. Atwell, G. J., G. W. Rewcastle, B. C. Baguley and W. A. Denny (1990) Potential antitumor agents. 60. Relationships between structure and in vivo colon 38 activity for 5-substituted 9-oxoxanthene-4-acetic acids. *J. Med. Chem.* **33**, 1375–1379.
32. Ibrom, W. G. A. and A. W. Frahm (1997) Synthesis and antimycobacterial activity of nitroxanthones 1st communication: synthesis and differential scanning calorimetry analysis. *Arzneim.-Forsch./Drug Res.* **47**, 662–667.
33. Ignatushchenko, M. V., R. W. Winter, H. P. Bächinger, D. V. Hinrichs and M. K. Riscoe (1997) Xanthenes as antimalarial agents; studies of a possible mode of action. *FEBS Lett.* **409**, 67–73.
34. Lin, C.-N., H.-K. Hsieh, S.-J. Liou, H.-H. Ko, H.-C. Lin, M.-I. Chung, F.-N. Ko, H.-W. Liou and C.-M. Teng (1996) Synthesis and antithrombotic effect of xanthone derivatives. *J. Pharm. Pharmacol.* **48**, 887–890.
35. Lin, C.-N., S.-J. Liou, T.-H. Lee, Y.-C. Chuang and S.-J. Won (1996) Xanthone derivatives as potential anti-cancer drugs. *J. Pharm. Pharmacol.* **48**, 539–544.
36. Liou, S.-S., W.-L. Shieh, T.-H. Cheng, S.-J. Won and C.-N. Lin (1993) γ -Pyrone compounds as potential anti-cancer drugs. *J. Pharm. Pharmacol.* **45**, 791–794.
37. Wang, T.-C., Y.-L. Chen, C.-C. Tzeng, S.-S. Liou, Y.-L. Chang and C.-M. Teng (1996) 137. Antiplatelet α -methylidene- γ -butyrolactones: synthesis and evaluation of quinoline, flavone, and xanthone derivatives. *Helv. Chim. Acta.* **79**, 1620–1626.
38. Gullard, J. M. and R. Robinson (1925) Synthetic experiments in the naphthyridine groups. *J. Chem. Soc.* **127**, 1493–1503.
39. Goldberg, A. A. and H. A. Walker (1953) Synthesis of diaminoxanthones. *J. Chem. Soc.* 1348–1357.
40. Mann, F. G. and J. H. Turnbull (1951) Xanthenes and thioxanthenes. I. The synthesis of 2- and 3-dialkylaminoalkylamino derivatives. *J. Chem. Soc.* 747–756.
41. Bohne, C., R. W. Redmond and J. C. Scaiano (1991) Use of photophysical techniques in the study of organized assemblies. In *Photochemistry in Organized & Constrained Media* (Edited by V. Ramamurthy), pp.79–132. VCH Publishers, New York.
42. Dawson, W. R. and M. W. Windsor (1968) Fluorescence yields of aromatic compounds. *J. Phys. Chem.* **72**, 3251–3260.
43. Eaton, D. F. (1990) Recommended methods for fluorescence decay analysis. *Pure Appl. Chem.* **62**, 1631–1648.
44. McGhee, J. D. and P. H. von Hippel (1974) Theoretical aspects of DNA-protein interactions: co-operative and non-co-operative binding of large ligands to a one-dimensional homogenous lattice. *J. Mol. Biol.* **86**, 469–489.
45. Ireland, J. F. and P. A. H. Wyatt (1972) Excited singlet and triplet pK values of xanthone in aqueous solution. *J. Chem. Soc., Faraday Trans. 1.* **68**, 1053–1058.
46. Pownall, H. J. and J. R. Huber (1971) Absorption and emission spectra of aromatic ketones and their medium dependence. Excited states of xanthone. *J. Am. Chem. Soc.* **93**, 6429–6436.
47. Abdullah, K. A. and T. J. Kemp (1986) Solvatochromic effects in the fluorescence and triplet-triplet absorption spectra of xanthone, thioxanthone and N-methylacridone. *J. Photochem. Photobiol. A: Chem.* **32**, 49–57.
48. Syromyatnikov, V. G., V. M. N. Yashchuk, T. Y. Ogul'chansky, O. O. Novikova, Y. P. Piryatinsky and O. Y. Kolendo (1999) Nature of 2-aminoxanthone fluorescence. *J. Fluoresc.* **9**, 93–98.
49. Boch, R., M. K. Whittlesey and J. C. Scaiano (1994) Laser-induced photoionization of aromatic ketones in anionic micellar solutions. *J. Phys. Chem.* **98**, 7854–7857.
50. Elisei, F., G. Favaro and H. Gömer (1991) Ion-forming processes on 248 nm laser excitation of benzophenone in aqueous solution: a time-resolved absorption and conductivity study. *J. Photochem. Photobiol. A: Chem.* **59**, 243–253.
51. Okano, L. T., R. Ovans, V. Zunic, J. N. Moorthy and C. Bohne (1999) Effect of cyclodextrin complexation on the photochemistry of the lignin model α -guaiacoxycetoveratrone. *Can. J. Chem.* **77**, 1356–1365.
52. Janata, E. and R. H. Schuler (1982) Rate constant for scavenging e_{aq}^- in N_2O -saturated solutions. *J. Phys. Chem.* **86**, 2078–2084.
53. Murov, S. L., I. Carmichael and G. L. Hug (1993) *Handbook of Photochemistry*. Marcel Dekker, New York.
54. Carmichael, I. and G. L. Hug (1986) Triplet-triplet absorption spectra of organic molecules in condensed phases. *J. Phys. Chem. Ref. Data* **15**, 1–250.
55. Treinin, A. and E. Hayon (1976) Quenching of triplet states by inorganic ions. Energy transfer and charge transfer mechanisms. *J. Am. Chem. Soc.* **98**, 3884–3891.
56. Almgren, M., F. Grieser and J. K. Thomas (1979) Dynamic and static aspects of solubilization of neutral arenes in ionic micellar solutions. *J. Am. Chem. Soc.* **101**, 279–291.
57. Ju, C. and C. Bohne (1996) Dynamics of probe complexation to bile salt aggregates. *J. Phys. Chem.* **100**, 3847–3854.

58. Rinco, O., M. H. Kleinman and C. Bohne (2001) Reactivity of benzophenones in the different binding sites of sodium cholate aggregates. *Langmuir* **17**, 5781–5790.
59. Rinco, O., M.-C. Nolet, R. Ovans and C. Bohne (2003) Probing the binding dynamics to sodium cholate aggregates using naphthalene derivatives as guests. *Photochem. Photobiol. Sci.* **2**, 1140–1151.
60. Barros, T. C., K. Stefaniak, J. F. Holzwarth and C. Bohne (1998) Complexation of naphthylethanol with β -cyclodextrin. *J. Phys. Chem. A* **102**, 5639–5651.
61. Turro, N. J., T. Okubo and C.-J. Chung (1982) Analysis of static and dynamic host-guest associations of detergents with cyclodextrins via photoluminescence methods. *J. Am. Chem. Soc.* **104**, 1789–1794.
62. Hirakawa, K., M. Yoshida, S. Oikawa and S. Kawanishi (2003) Base oxidation at the 5' site of GG sequence in double-stranded DNA induced by UVA in the presence of xanthone analogues: relationship between the DNA-damaging abilities of photosensitizers and their HOMO energies. *Photochem. Photobiol.* **77**, 349–355.
63. Inoue, H., M. Hida, N. Nakashima and K. Yoshihara (1982) Picosecond fluorescence lifetimes of anthraquinone derivatives. Radiationless deactivation via intra- and intermolecular hydrogen bonds. *J. Phys. Chem.* **86**, 3184–3186.
64. Moog, R. S., N. A. Burozski, M. M. Desai, W. R. Good, C. D. Silvers, P. A. Thompson and J. D. Simon (1991) Solution photophysics of 1- and 3-aminofluorenone: the role of inter- and intramolecular hydrogen bonding in radiationless deactivation. *J. Phys. Chem.* **95**, 8466–8473.
65. Biczók, L., T. Bérces and H. Inoue (1999) Effects of molecular structure and hydrogen bonding on the radiationless deactivation of singlet excited fluorenone derivatives. *J. Phys. Chem. A* **103**, 3837–3842.
66. Biczók, L., T. Bérces and H. Linschitz (1997) Quenching processes in hydrogen-bonded pairs: interactions of excited fluorenone with alcohols and phenols. *J. Am. Chem. Soc.* **119**, 11071–11077.
67. Flom, S. R. and P. F. Barbara (1985) Proton transfer and hydrogen bonding in the internal conversion of S_1 anthraquinones. *J. Phys. Chem.* **89**, 4489–4494.